Available online at www.sciencedirect.com
SCIENCE DIRECT®
Journal of Solid State Chemistry 171 (2003) 257–261
JOURNAL OF SOLID STATE CHEMISTRY
http://elsevier.com/locate/jssc

Selective distribution of dopants among MO_6 octahedra in $RbTi_{0.927}Nb_{0.056}Er_{0.017}OPO_4$: a neutron diffraction study

J.J. Carvajal,[a] J.L. García-Muñoz,[b] R. Solé,[a] Jna. Gavaldà,[a] J. Massons,[a] M. Aguiló,[a] and F. Díaz[a,*]

[a] *Física i Cristal-lografia de Materials, Universitat Rovira i Virgili, Pl. Imperial Tarraco, 1, 43005 Tarragona, Spain*
[b] *Institut de Ciència de Materials de Barcelona, C.S.I.C., Campus universitari de Bellaterra, E-08193 Bellaterra, Spain*

Received 6 May 2002; received in revised form 26 June 2002; accepted 10 July 2002

Abstract

Codoping $RbTiOPO_4$ crystals (RTP) with Er^{3+} and Nb^{5+} is interesting in order to merge the rare earth ion photoluminescence and the non-linear optical properties of the matrix, favouring self-induced effects. Using RTP crystals doped with Nb^{5+}, a concentration of Er^{3+} similar to that obtained in other laser matrices was achieved. In this work, the structure of $RbTi_{0.927}Nb_{0.056}Er_{0.017}OPO_4$ has been thoroughly studied by high-resolution neutron diffraction. Particular attention has been paid to the positions occupied by Er^{3+} and Nb^{5+} in the structure and the distortion of their respective coordination polyhedra. Finally, the second-harmonic generation efficiency of the sample has been determined and compared to other members of the family.

Keywords: Powder neutron diffraction; Non-linear optics; Second-harmonic generation; $KTiOPO_4$; $RbTiOPO_4$

1. Introduction

Potassium titanyl phosphate, $KTiOPO_4$ (KTP) is the most well known member of the family of compounds with formula $MM'OXO_4$ (M = K, Rb, Tl, Na or Cs, M' = Ti, Ge, Sn and X = P or As) or partial substitution in M and M' by two or more different cations [1]. All members of this family are orthorhombic, biaxial crystals and crystallize in the non-centrosymmetric space group $Pna2_1$ (point group $mm2$) [2] and many of them are of interest because their non-linear optical (NLO) properties [3].

The main reason for which these crystals show NLO properties seems to be the deformation of the $M'O_6$ octahedra: more distorted these octahedra are, higher is the second-harmonic generation (SHG) efficiency of the material [4]. Other authors have also claimed that the MO_8 or MO_9 groups can also play a role in the efficiency of this effect [5].

Doping these crystals with lanthanide ions is interesting because the ion photoluminescence and the NLO properties of the matrix can be merged to achieve self-induced effects. In previous works [6–8], we showed that using RTP crystals doped with Nb^{5+} as a matrix to host Er^{3+}, a concentration of this ion similar to that obtained in other laser matrices was achieved. Er^{3+} is interesting because of its much-studied emission around 1.5 μm, useful in optical communications at long distances due to the important losses in silica fibres in this region [9].

In this work, we report on the crystal structure of $RbTi_{0.927}Nb_{0.056}Er_{0.017}OPO_4$, paying particular attention to the positions occupied by dopant cations, Er and Nb, in the unit cell. In addition, we also report measurements of its SHG efficiency. The results are discussed in comparison with other members of this family of materials and their NLO properties.

2. Experimental procedure

$RbTi_{0.927}Nb_{0.056}Er_{0.017}OPO_4$ single crystals were grown by the high-temperature flux method from a solution with a molar composition Rb_2O–P_2O_5–TiO_2–Nb_2O_5–Er_2O_3 = 42.0–28.0–27.6–1.5–0.9, by spontaneous

*Corresponding author. Fax: +34-977-55-95-63.
E-mail address: diaz@quimica.urv.es (F. Díaz).

0022-4596/03/$ - see front matter © 2003 Elsevier Science (USA). All rights reserved.
doi:10.1016/S0022-4596(02)00172-X

nucleation on a Pt wire, as described elsewhere [6]. Rb_2CO_3, $NH_4H_2PO_4$, TiO_2, Nb_2O_5 and Er_2O_5 pro analysis (p.a.) were used as initial reagents and mixed in the desired ratios. The quality of the sample was first checked by X-ray powder diffraction in a Siemens D5000 powder diffractometer in a $\theta-\theta$ configuration using Bragg–Brentano geometry. These measurements show that the sample was single phase.

The crystals obtained were cleaned and analysed by electron probe microanalyses (EPMA) to obtain the concentration of Er and Nb. A CAMECA SX-50 was used, operating in wavelength dispersive mode. The concentration of Rb, Ti, P, Nb and O were analysed at 30 nA electron current, while the concentration of Er was measured at 100 nA. In all cases, the accelerating voltage was maintained at 25 kV. The raw intensities were corrected for dead time, background and matrix effects using the PAP correction procedure [10].

Neutron powder diffraction (NPD) measurements were carried out at the D2B high-resolution diffractometer at the Institut Laue Langevin (Grenoble, France). This diffractometer is equipped with a bank of 64 detectors separated by 2.5° in 2θ, spanning and an angular range of 160°. The wavelength used was 1.594 Å and the counting time was about 3 h to have the desired statistics over the angular range 0–160° in 2θ. The pattern obtained at room temperature in the high-flux mode was of good quality. We used the Rietveld method to analyse the neutron diffraction data, using the refinement program FULLPROF [11]. The sample was prepared from powdered single crystals of $RbTi_{0.927}Nb_{0.056}Er_{0.017}OPO_4$ and graded between 5 and 20 μm using standard sieves. The stoichiometry of the sample was determined from the results of EPMA.

The SHG efficiency of $RbTi_{0.927}Nb_{0.056}Er_{0.017}OPO_4$ was analysed by powder technique [12]. The sample was prepared in the same conditions of the NPD measurements. The powder was illuminated with a YAG:Nd pulsed laser. We estimated the fundamental power by measuring the 1064 nm energy reflected by the sample. On the other hand, the backscattered harmonic power generated by the sample was collected with a lens and focused on a Si detector. These signals were analysed using a digital oscilloscope, and we used the ratio between the two maxims to describe the SHG efficiency. This method does not allow to measure the SHG absolute efficiency of the samples; so this parameter was compared with that of pure KTP, which is well established in the literature [13].

3. Results and discussion

3.1. Structural characterization

The $RbTi_{0.927}Nb_{0.056}Er_{0.017}OPO_4$ sample was impurity free. This crystal is isostructural to KTP and RTP, as shown by the X-ray powder diffraction patterns taken in the first stage of the crystal growth experiments [6]. Then, the structural refinements of the NPD data were performed in the orthorhombic $Pna2_1$ group, using as starting model the structure for a RTP:Nb crystal resolved at room temperature by our own group [14].

In this structure, there are two crystallographic independent Ti positions (Ti(1) and Ti(2)), two P and two Rb positions, as well as 10 non-equivalent oxygen atoms. All these atoms occupy general positions. A careful analysis of high-resolution NPD data allowed us to thoroughly study fine structural details such as oxygen positions and, in particular, to determine the dopants location. A pseudo-Voigt profile function corrected for asymmetry and a six-parameter polynomial function reproducing the background were used in the refinements.

Table 1 shows the room temperature cell parameters, refined atomic coordinates and isotropic temperature factors as well as the final reliability factors obtained from NPD data. Fig. 1 illustrates the agreement between observed and calculated NPD profiles.

Our main purpose was obtaining reliable information on the distribution of the small concentration of Nb^{5+} and Er^{3+} cations in the structure. As a starting point, we used a random distribution of Nb^{5+} and Er^{3+} among Ti^{4+} sites and performed, for different models of dopants distribution, different sets of Rietveld refinements of the NPD data. Refinements show that Nb and Er go only to Ti sites in the present structure. In addition, we checked for the possibility of rubidium or oxygen vacancies. We found all the atomic positions, including rubidium or oxygen sites, fully occupied, with a resolution of around 1%, in contrast with some potassium vacancies reported for the Nb-doped $KTiOPO_4$ single crystal [15].

When we perform Rietveld refinements with random substitution of Nb and Er among the two Ti sites, the agreement factors are: $R_{wp} = 6.82\%$, $R_f = 4.74\%$ and $R_{Bragg} = 6.20\%$. In contrast, with an inhomogeneous distribution of the dopants, the reliability factors clearly improve. The refinements always converge to the same scenario: Nb cations are only found substituting Ti(1) positions, at the centre of the $Ti(1)O_6$ octahedra. In addition, we were able to refine the occupation factors of Nb and Er freely, with the only constraints that Ti octahedra are fully occupied, and have no vacants, and the concentration of these cations correspond to that obtained by EPMA analyses. Table 2 shows the values to which the occupation factors converge. In the case of Er, the refinements converge to the occupations 0.014(4) and 0.020(4) for Er(1) and Er(2), respectively. According to the errors, an undistinguishable situation to having Er equally distributed between Ti(1) and Ti(2) (a fraction 0.017 in each octahedral) can be assumed.

Table 1
Cell parameters, refined atomic coordinates and isotropic temperature factors from neutron data at RT. All atoms are in general ($x\,y\,z$) position ($Pna2_1$ space group)

Cell parameters				
a (Å) = 12.9716(2)	b (Å) = 6.5069(1)	c (Å) = 10.5740(2)	V (Å^3) = 892.49(2)	
Atom	x	y	z	B_{iso} (Å^2)
Ti(1)	0.373(1)	0.491(5)	0.437(3)	0.5(2)
Ti(2)	0.247(2)	0.268(3)	0.692(2)	0.5(2)
P(1)	0.499(1)	0.335(1)	0.695(2)	0.61(8)
P(2)	0.1812(5)	0.495(3)	0.946(2)	0.61(8)
Rb(1)	0.3864(8)	0.786(1)	0.765(1)	1.86(9)
Rb(2)	0.1058(9)	0.690(1)	0.519(1)	1.87(9)
O(1)	0.4837(8)	0.484(2)	0.588(1)	0.59(2)
O(2)	0.512(1)	0.456(1)	0.821(1)	0.59(2)
O(3)	0.398(1)	0.201(2)	0.717(1)	0.59(2)
O(4)	0.594(1)	0.197(2)	0.677(1)	0.59(2)
O(5)	0.110(1)	0.311(2)	0.981(1)	0.60(2)
O(6)	0.116(1)	0.690(2)	0.921(1)	0.60(2)
O(7)	0.251(1)	0.542(2)	0.064(1)	0.60(2)
O(8)	0.254(1)	0.458(2)	0.834(1)	0.60(2)
OT(1)	0.223(1)	0.960(2)	0.079(1)	0.60(2)
OT(2)	0.222(1)	0.045(2)	0.827(1)	0.60(2)

Reliability factors: $\chi^2 = 1.65\%$, $R_p = 5.39\%$, $R_{wp} = 6.82\%$, $R_f = 4.74\%$, $R_{Bragg} = 6.20\%$.

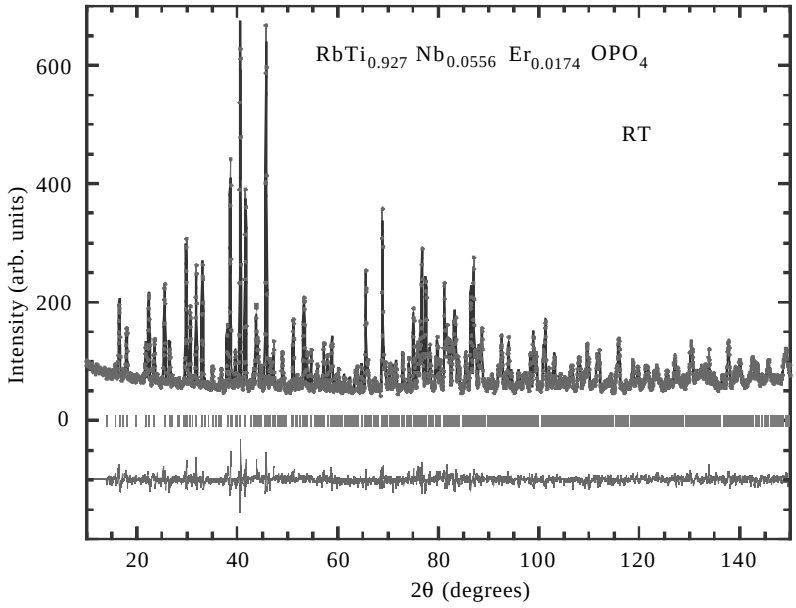

Fig. 1. Refined neutron diffraction pattern of $RbTi_{0.927}Nb_{0.056}Er_{0.017}OPO_4$ showing the observed D2B data (points), calculated (full line) and difference (bottom) Rietveld profiles at RT.

Table 3 lists the bond distances in $Ti(1)O_6$ and $Ti(2)O_6$ octahedra in the $RbTi_{0.927}Nb_{0.056}Er_{0.017}OPO_4$ structure. In this crystal, the characteristic long and short Ti–O bond distances in the structure of KTP family are maintained. In this family of compounds, $Ti(1)O_6$ octahedra are slightly expanded with respect to $Ti(2)O_6$, namely, the volume defined by the latter is lower than the former. At this point, we recall that the ionic radii of Nb^{5+} and Er^{3+} ions are rather different: 0.64 (Nb^{5+}) and 0.881 Å (Er^{3+}), Nb^{5+} ions being more similar to Ti^{4+} than Er^{3+} ions. Regarding these ionic sizes, the tendency of Nb^{5+} ions to occupy Ti(1) sites (not observed for the more voluminous Er^{3+} cations) is not justified sterically and its origin is very likely electrostatic [15]. It is to be noted that there is one individual bond (Ti(1)–O5) that has lengthened quite a lot in the doped crystal: from 2.076 Å (pure RTP) to 2.13 Å (present sample). In the $Ti(2)O_6$ units, Ti(2)–OT(1) also increases from 1.73 to 1.77. However, if we compare the resulting Ti–O distances in $RbTi_{0.927}$

Table 2
Occupation factors at the two Ti sites in $RbTi_{0.927}Nb_{0.056}Er_{0.017}OPO_4$ determined from high resolution neutron diffraction data. Distribution of Nb^{5+} and Er^{3+} ions among the two different TiO_6 octahedra

Atom	Occupation factor
Ti(1)	0.871(6)
Nb(1)	0.111(6)
Er(1)	0.017(4)
Ti(2)	0.983(6)
Nb(2)	0.000(6)
Er(2)	0.017(4)

Table 3
Comparison of $Ti(1)O_6$ and $Ti(2)O_6$ octahedra as determined from neutron diffraction: main Ti–O bond lengths (Å)

Ti(1)–O(1)	2.15(3)	Ti(2)–O(3)	2.03(3)
Ti(1)–O(2)	1.96(3)	Ti(2)–O(4)	2.00(2)
Ti(1)–O(5)	2.14(4)	Ti(2)–O(7)	2.00(2)
Ti(1)–O(6)	1.97(4)	Ti(2)–O(8)	1.95(3)
Ti(1)–OT(1)	1.96(3)	Ti(2)–OT(1)	1.77(2)
Ti(1)–OT(2)	1.73(3)	Ti(2)–OT(2)	2.06(2)
⟨Ti(1)–O⟩	1.985	⟨Ti(2)–O⟩	1.968

$Nb_{0.056}Er_{0.017}OPO_4$ with those in undoped RTP [16], within our resolution, we do not appreciate changes in the average Ti(1)–O and Ti(2)–O distances of the octahedra.

3.2. Second harmonic generation

The SHG efficiency (η) was defined as the ratio between the powers of the pumping beam (1064 nm) and the green one (532 nm). It is convenient as well to refer the result of our measurements to KTP, now that the parameters of this material are well established in the literature [13]. In our case, we have found $\eta_{sample}/\eta_{KTP} = 0.68$. This value is slightly lower than that of pure RTP ($\eta_{RTP}/\eta_{KTP} = 0.73$), and clearly lower than that previously found for a sample of RTP doped only with a similar concentration of Nb [6] ($\eta/\eta_{KTP} = 1.23$ for $RbTi_{0.96}Nb_{0.04}OPO_4$). The observed reduction in the SHG efficiency of our sample can be mainly attributed to the presence of Er in the sample. As it is well known, the $^2H_{15/2}$ manifold of this ion allows an important absorption of light in the green region [6–8]. However, our measurements show that this absorption does not cause a dramatic decrease of η, and we thus conclude that the NLO properties of our Nb,Er-doped crystal are only moderately reduced with respect to the properties of RTP crystal.

Although this decrease in the η could be easily explained by the green absorption of Er^{3+}, both TiO_6 octahedra in this crystal are less distorted when comparing with RTP. According to the expression $|d_{equat}/d_{apic} - 1| \times 10^4$, where d_{equat} is the mean distance of the four Ti–O bonds in the equatorial plane of the octahedra and d_{apic} is the mean distance of the two apical Ti–O bonds, the distortion of the $Ti(1)O_6$ and $Ti(2)O_6$ octahedra in $RbTi_{0.927}Nb_{0.056}Er_{0.017}OPO_4$ take values of 521 and 369, respectively, while the same parameters in RTP are 527 and 443, respectively. Then, it seems that the more distorted the TiO_6 octahedra, the higher is the η of the material.

4. Conclusions

High-resolution neutron powder diffraction measurements were carried out to investigate the distribution of the small concentration of Nb and Er cations in the crystal structure of $RbTi_{0.927}Nb_{0.056}Er_{0.017}OPO_4$. We confirmed that Nb and Er only go to Ti sites. However, careful analysis of the data rules out a random distribution of dopants among Ti sites. We have been able to refine the occupation factors of Nb and Er freely, with the only restriction that Ti octahedra are fully occupied and the concentrations of Nb, Er and Ti are those corresponding to the EPMA analyses. Rietveld refinements confirmed that in this new crystal, Nb^{5+} cations exclusively substitute Ti(1) sites. This is in contrast with Er^{3+} cations, which were found to substitute Ti atoms of $Ti(1)O_6$ and $Ti(2)O_6$ octahedra with the same probability. As expected, codoping RTP crystals with Nb and Er result in a decrease of the second harmonic generation efficiency. But we have observed just a moderate reduction of η in $RbTi_{0.927}Nb_{0.056}Er_{0.017}OPO_4$, this crystal having an SHG efficiency very similar to pure RTP.

Acknowledgments

The authors would like to thank the ILL for making available the beam time, and financial support by the OCYT (PB97-1175 project), CICyT (MAT99-1077 and FIT–070000-2001–477) and DURSI (2001SGR 317, GRQ95-8029, PICS2001-22). J.J. Carvajal would also like to acknowledge a fellowship from the Generalitat de Catalunya (2000FI 00633 URV APTIND).

References

[1] M.E. Hagerman, K.R. Poeppelmeier, Chem. Mater. 7 (1995) 602–621.
[2] L.K. Cheng, L.T. Cheng, J. Galperin, P.A. Morris Hotsenpiller, J.D. Bierlein, J. Cryst. Growth. 137 (1994) 107–115.
[3] F.C. Zumsteg, J.D. Bierlein, T.E. Gier, J. Appl. Phys. 47 (1976) 4980–4985.

[4] V.I. Voronkova, V.K. Yanovskii, N.I. Sorokina, I.A. Verin, V.I. Simonov, Crystallogr. Rep. 38 (1993) 662–664.
[5] D.F. Xue, S.Y. Zhang, Appl. Phys. Lett. 70 (1997) 943–945.
[6] J.J. Carvajal, V. Nikolov, R. Solé, Jna. Gavaldá, J. Massons, M. Rico, C. Zaldo, M. Aguiló, F. Díaz, Chem. Mater. 12 (2000) 3171–3180.
[7] J.J. Carvajal, R. Solé, Jna. Gavaldá, J. Massons, M. Rico, C. Zaldo, M. Aguiló, F. Díaz, J. Alloys Compds. 323–324 (2001) 231–235.
[8] J.J. Carvajal, R. Solé, Jna. Gavaldá, J. Massons, M. Aguiló, F. Díaz, Cryst. Growth Design 1 (2001) 479–484.
[9] G. Dominiak-Dzik, S. Golab, I. Pracka, W. Ryba-Romanowski, Appl. Phys. A 58 (1994) 551–555.
[10] J.L. Pouchou, F. Pichoir, Rech. Aerosp. 3 (1984) 13.
[11] J. Rodríguez-Carvajal, Physica B 192 (1993) 55.
[12] S.K. Kurtz, T.T. Perry, J. Appl. Phys. 39 (1968) 3798–3813.
[13] V.G. Dmitriev, G.G. Gurzadyan, D.N. Nikogosyan, Handbook of Nonlinear Optical Materials, Springer, 1991.
[14] Física i Cristal·lografia de Materials, unpublished material.
[15] P.A. Thomas, B.E. Watts, Solid State Commun. 73 (1990) 97–100.
[16] P.A. Thomas, S.C. Mayo, B.E. Watts, Acta Crystallogr. B48 (1992) 401–407.